Monthly Notices
of the
ROYAL ASTRONOMICAL SOCIETY

MNRAS **475,** L1–L5 (2018)
Advance Access publication 2017 December 5

doi:10.1093/mnrasl/slx199

The effect of pair cascades on the high-energy spectral cut-off in gamma-ray bursts

Ramandeep Gill[1,2]★ and Jonathan Granot[1,3]★

[1]*Department of Natural Sciences, The Open University of Israel, 1 University Road, PO Box 808, Raanana 4353701, Israel*
[2]*Physics Department, Ben-Gurion University, PO Box 653, Beer-Sheva 84105, Israel*
[3]*Department of Physics, The George Washington University, Washington, DC 20052, USA*

Accepted 2017 November 28. Received 2017 November 23; in original form 2017 October 30

ABSTRACT

The highly luminous and variable prompt emission in gamma-ray bursts (GRBs) arises in an ultra-relativistic outflow. The exact underlying radiative mechanism shaping its non-thermal spectrum is still uncertain, making it hard to determine the outflow's bulk Lorentz factor Γ. GRBs with spectral cut-off due to pair production ($\gamma\gamma \rightarrow e^+e^-$) at energies $E_c \gtrsim 10\,\mathrm{MeV}$ are extremely useful for inferring Γ. We find that when the emission region has a high enough compactness, then as it becomes optically thick to scattering, Compton downscattering by non-relativistic $e^{\pm}$-pairs can shift the spectral cut-off energy well below the self-annihilation threshold, $E_{\rm sa} = \Gamma m_e c^2/(1+z)$. We treat this effect numerically and show that Γ obtained assuming $E_c = E_{\rm sa}$ can underpredict its true value by as much as an order of magnitude.

Key words: opacity – plasmas – radiative transfer – relativistic processes – gamma-ray burst: general.

1 INTRODUCTION

The GRB prompt emission is typically highly variable, consisting of multiple spikes spanning a wide range of widths, $\Delta T \sim 10^{-3} - 1\,\mathrm{s}$ (e.g. Fishman & Meegan 1995). In the GRB central engine frame (CEF; cosmological rest frame of source) at redshift z, the variability time is $T_v = \Delta T/(1+z)$. For a Newtonian source, light travel effects imply a source size $R \lesssim cT_v$. Since GRBs are extremely luminous sources, with typical energy fluxes $F \sim 10^{-6}\,\mathrm{erg\,cm^{-2}\,s^{-1}}$, and luminosity distances $d_{\rm L} \sim 10^{28}\,\mathrm{cm}$, a typical photon near the νF_ν peak with energy $E \sim E_{\rm pk} \sim m_e c^2$ would see a huge optical depth $\tau_{\gamma\gamma}(E) \sim \sigma_{\rm T} f_{\gamma\gamma}(E) n_\gamma R \sim 10^{13}$ to pair production, $\gamma\gamma \rightarrow e^+e^-$ (Piran 1999), where $\sigma_{\rm T}$ is the Thomson cross-section, n_γ is the photon number density, and $f_{\gamma\gamma}(E)$ is the fraction of photons that can pair produce with the test photon of energy E. This would imply a huge compactness $\ell \equiv \sigma_{\rm T} U_\gamma R/m_e c^2$ (Thomson optical depth of pairs if all photons pair produce), where U_γ is the radiation field energy density, which would result in a nearly blackbody spectrum, in stark contrast with the observed GRB non-thermal spectrum.

The solution to this so-called 'compactness-problem', is that the emission region must be moving towards us ultrarelativistically with $\Gamma \gtrsim 10^2$ (Ruderman 1975; Goodman 1986; Paczyński 1986; Rees & Mészáros 1992). This implies: (i) Doppler factor: a blueshift such that the observed energy of photons $E = \Gamma E'/(1+z)$ (primed quantities are measured in the outflow's comoving rest frame) is higher by a factor of $\sim\Gamma$ than that in the comoving frame and (ii) the emission radius can be larger by a factor of $\sim\Gamma^2$, and assume a value of up to[1] (see Kumar & Zhang 2015, for a review)

$$R \approx 2\Gamma^2 cT_v = 6\times 10^{13}\Gamma_2^2 T_{v,-1}\,\mathrm{cm}. \quad (1)$$

Effect (i) increases the threshold to $\gamma\gamma$-annihilation in terms of the observed photon energy (i.e. decreases $f_{\gamma\gamma}(E)$) while effect (ii) reduces the required n_γ. For a power-law photon spectrum $\mathrm{d}N/\mathrm{d}E \propto E^{-\alpha}$, $\tau_{\gamma\gamma}(E) \propto L_0 E^{\alpha-1}/\Gamma^{2\alpha} R \rightarrow L_0 E^{\alpha-1}/\Gamma^{2\alpha+2} T_v$ (assuming equation 1; Granot, Cohen-Tanugi & do Couto E Silva 2008, hereafter G08), where $L_0 = EL_{\rm E}(E = m_e c^2)$.

Depending on Γ, and other intrinsic parameters (e.g. Vianello et al. 2017) such as the radiated power L_γ, T_v, and R if $R \neq R(T_v)$ (see e.g. Gupta & Zhang 2008), the energy where the outflow becomes opaque to $\gamma\gamma$ absorption can be pushed to $E \gg E_{\rm pk}$, at which point the non-thermal spectrum is either exponentially suppressed or manifests a smoothly broken power law (G08).

The existence of a high-energy spectral cut-off occurring due to intrinsic $\gamma\gamma$-opacity has important implications. Since the bulk-Γ of the outflow is hard to obtain and observations of the highest energy photons without a cut-off provide only a lower limit, measuring a spectral cut-off instead yields a direct estimate (e.g. Fenimore, Epstein & Ho 1993; Woods & Loeb 1995; Baring & Harding 1997; Lithwick & Sari 2001; Razzaque et al. 2004; Baring 2006; Murase & Ioka 2008; G08; Gupta & Zhang 2008). So far, a high-energy cut-off has only been observed in a handful of sources, e.g. GRB 090926A (Ackermann et al. 2011) and GRBs 100724B

★ E-mail: rsgill.rg@gmail.com (RG); granot@openu.ac.il (JG)

[1] In this work, we adopt the convention $Q_x = Q/10^x$ (c.g.s. units).

© 2017 The Author(s)
Published by Oxford University Press on behalf of the Royal Astronomical Society

Downloaded from https://academic.oup.com/mnrasl/article-abstract/475/1/L1/4693845
by OPEN UNIVERSITY user
on 17 January 2018

& 160409A (Vianello et al. 2017, for a more complete list see Tang et al. 2015). Most analytic works employ a simple one-zone model with an isotropic (comoving) radiation field (e.g. Lithwick & Sari 2001, hereafter LS01) and obtain Γ from the condition that the cut-off energy E_c is given by $E_c = E_1$, where $\tau_{\gamma\gamma}(\Gamma, E_1) \equiv 1$. However, detailed analytic and numerical treatments of the $\gamma\gamma$-opacity near the dissipation region, which account for the space, time and direction dependence of the radiation field, by G08 and Hascoët et al. (2012), respectively, have shown that the actual estimate of Γ should be lower by a factor of $\sim$2.

What was neglected so far in all works is the effect of $e^{\pm}$-pairs that are produced, and in particular pair cascades, on the scattering opacity and further redistribution of the radiation field energy by Comptonization. Its neglect stems from the inherent non-linearity associated with developing pair cascades, which is hard to treat self-consistently using a semi-analytic approach and requires a numerical treatment. Highly luminous compact sources with $\tau_{\gamma\gamma} \gg 1$ naturally develop high Thomson scattering optical depth $\tau_T \gg 1$ due to resultant $e^{\pm}$-pairs that can significantly modify the source spectrum via Comptonization (Guilbert, Fabian & Rees 1983).

Time-dependent numerical models of GRB prompt emission phase (e.g. Pe'er & Waxman 2005; Vurm, Beloborodov & Poutanen 2011; Gill & Thompson 2014) self-consistently account for $\gamma\gamma$ annihilation, automatically produce the spectral attenuation at comoving energies $E' > m_e c^2$, and account for the enhanced scattering opacity due to pair production. Here, we use a time-dependent kinetic code to study how $e^{\pm}$-pairs affect the position of the cut-off that arises due to $\gamma\gamma$-opacity. The code includes Compton scattering, cyclo-synchrotron emission and self-absorption, pair-production and annihilation, Coulomb interaction, adiabatic cooling, and photon escape. In Section 2, we review a simple one-zone model of $\gamma\gamma$ annihilation opacity and derive estimates for the scattering optical depth of $e^{\pm}$-pairs in the optically thick and thin regimes. We construct a general model of a magnetized dissipative relativistic outflow in Section 3 in which the prompt emission is attributed to synchrotron emission by relativistic electrons and $e^{\pm}$-pairs. In Section 4, we discuss the implication of our results.

2 SCALING RELATIONS FROM A ONE-ZONE MODEL

We consider a simple *one-zone* model where the emission region is uniform with an isotropic radiation field (in its comoving frame). We denote dimensionless photon energies by $x \equiv E/m_e c^2$. The observed prompt emission photon-number spectrum at energies above the νF_ν-peak, $x_{pk} = E_{pk}/m_e c^2$, can be described by a power law,

$$\frac{dN}{dA dT dx} = N_0 \left(\frac{x}{x_0}\right)^{\beta}, \qquad x_{pk} < x_0 < x < x_{max}, \tag{2}$$

where $dA \to 4\pi d_L^2 (1+z)^{-2}$ for isotropic emission in the CEF, dT is the differential of the observed time, and N_0 [$\mathrm{cm^{-2}\,s^{-1}}$] is the normalization. It was shown by LS01 that for a given test photon energy, x_t, the optical depth due to $\gamma\gamma$-annihilation is

$$\tau_{\gamma\gamma} = (1+z)^{-2(1+\beta)} \hat{\tau} \Gamma^{2\beta-2} x_t^{-(1+\beta)}$$
$$\hat{\tau} = \frac{(11/180)\sigma_T d_L^2 N_0 x_0^{-\beta}}{c^2 \Delta T (-1-\beta)} = \frac{(11/180)\sigma_T \tilde{L}_0 x_0^{-(2+\beta)}}{4\pi c^2 \Delta T (-1-\beta)}, \tag{3}$$

where $\tilde{L}_0 \equiv L_0(x_0)/m_e c^2 = 4\pi d_L^2 x_0^2 N_0$ and $L_0(x_0)$ is the radiated isotropic equivalent luminosity in the CEF at $x = x_0$. This equation can be used to define the critical photon energy x_1 at which $\tau_{\gamma\gamma}(x_1) \equiv 1$. If the latter is indeed identified with the observed cut-off energy, $x_c \approx x_1$, this allows us to determine Γ,

$$\Gamma_{min} \equiv \Gamma(x_c) = (1+z)^{(-1-\beta)/(1-\beta)} \hat{\tau}^{1/(2-2\beta)} x_c^{(-1-\beta)/(2-2\beta)}. \tag{4}$$

If no spectral cut-off is observed and the power law extends up to an energy x_{max}, then equation (4) yields a lower limit $\Gamma_{min} = \Gamma(x_c = x_{max})$.

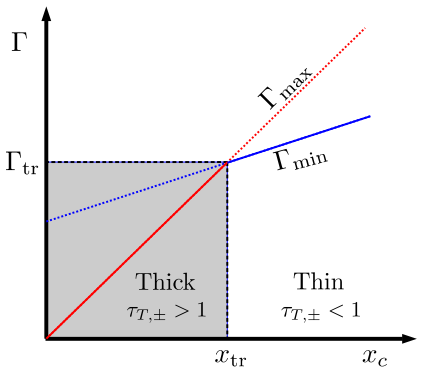

Figure 1. Schematic illustration of the two regimes – Thomson-thick and Thomson-thin – as defined in the text. The bulk Lorentz factor Γ of the emitting region is given by $\Gamma = \min(\Gamma_{max}, \Gamma_{min})$ and shown by solid lines.

In the comoving frame, test photons of energy x'_t have the highest probability to annihilate with other photons with energies just above the pair-production threshold, $x'_{an} \approx 1/x'_t$, since the cross-section decreases well above x'_{an} and vanishes below x'_{an}. Therefore, test photons of energy $x'_t > x'_{sa} = 1$ can self-annihilate whereas photons of energy $x'_t < x'_{sa}$ cannot. This has an important consequence for spectra with $\beta < -1$, which is generally the case for the prompt-GRB spectrum. In this case, $x dN/dx \propto x^{1+\beta}$ declines with photon energy x, and lower energy photons outnumber higher energy photons. This asymmetry in photon number defines two important regimes (shown in Fig. 1) as follows.

(i) *Thomson-Thick*: In this regime, $x'_1 < x'_{sa} = 1$ so that test photons in the energy range $x'_1 < x'_t < x'_{sa}$ initially face $\tau_{\gamma\gamma}(x'_t) > 1$, but they cannot self-annihilate. Instead, they can annihilate only with higher energy photons, $x' \geq x'_{an} \approx 1/x'_t$, but since they outnumber these higher energy photons they quickly annihilate almost all of them, which brings down $\tau_{\gamma\gamma}(x'_t)$ below 1. This results in a spectral cut-off at $x'_c = x'_{sa} = 1 \Leftrightarrow x_c = \Gamma/(1+z)$, i.e. in this regime $\Gamma = \Gamma_{max} = (1+z)x_c$. The notation Γ_{max} was chosen since it is the maximal possible Γ for a given cut-off energy x_c due to $\gamma\gamma$-annihilation alone.

Each annihilating photon-pair produces an $e^{\pm}$-pair, so the Thomson optical depth of the pairs (ignoring pair annihilation, PA) in this regime is $\tilde{\tau}_{T,\pm} = \frac{\sigma_T}{\sigma_{\gamma\gamma}} \tau_{\gamma\gamma}(x'_t = 1)$, where $\frac{\sigma_T}{\sigma_{\gamma\gamma}} \approx \frac{180}{11}$. Using equation (3),

$$\tilde{\tau}_{T,\pm} = \frac{180}{11} \frac{\hat{\tau} x_c^{\beta-3}}{(1+z)^4} = \frac{180}{11} \left[\frac{\Gamma_{min}(x_c)}{\Gamma_{max}(x_c)}\right]^{2(1-\beta)}, \tag{5}$$

where the last equality follows from equation (4). The ratio $\Gamma_{min}(x_c)/\Gamma_{max}(x_c)$ becomes unity at the transition energy (LS01),

$$x_{tr} = \left[(1+z)^{-4} \hat{\tau}\right]^{1/(3-\beta)} \Longleftrightarrow \Gamma_{tr} = \left[(1+z)^{-1-\beta} \hat{\tau}\right]^{1/(3-\beta)}, \tag{6}$$

which corresponds to $\Gamma_{tr} = (1+z)x_{tr}$. Therefore, for cut-off energies $x_c < x_{tr}$, $\Gamma_{min}(x_c) > \Gamma_{max}(x_c)$ and $\tilde{\tau}_{T,\pm} \gg 1$, when $\beta < -1$. In order to arrive at this result, the annihilation of $e^{\pm}$-pairs has been completely ignored, which would certainly modify the scattering opacity.

(ii) *Thomson-Thin*: In this regime $1 = x'_{sa} < x'_1$, so photons of energies $x'_{sa} < x'_t < x'_1$ can self-annihilate but have $\tau_{\gamma\gamma}(x'_t) < 1$ and

Downloaded from https://academic.oup.com/mnrasl/article-abstract/475/1/L1/4693845
by OPEN UNIVERSITY user
on 17 January 2018

only such a small fraction of them indeed annihilate. However, photons of energies $x'_{\rm t} > x'_1$ face $\tau_{\gamma\gamma}(x'_{\rm t}) > 1$ and almost all of them do annihilate, leading to a cut-off at $x'_{\rm c} = x'_1$. Hence, in this regime $\Gamma = \Gamma_{\rm min}$ (the minimal possible Γ for a given $x_{\rm c}$). Following the discussion above, here $\tilde{\tau}_{\rm T,\pm} \approx \frac{180}{11}\tau_{\gamma\gamma}(1/x'_1)$, or using equations (3) and (4),

$$\tilde{\tau}_{\rm T,\pm} = \frac{(x'_1)^{2+2\beta}}{11/180} = \frac{180}{11}\left[\frac{(1+z)^4}{\hat{\tau}\, x_{\rm c}^{\beta-3}}\right]^{\frac{1+\beta}{1-\beta}} = \frac{180}{11}\left[\frac{\Gamma_{\rm max}(x_{\rm c})}{\Gamma_{\rm min}(x_{\rm c})}\right]^{2+2\beta} . \quad (7)$$

This Thomson-thin regime corresponds to $x_{\rm c} > x_{\rm tr}$ and $\Gamma > \Gamma_{\rm tr}$, since here $\Gamma_{\rm min}(x_{\rm c}) < \Gamma_{\rm max}(x_{\rm c})$ which implies $\tilde{\tau}_{\rm T,\pm} < 1$, when $\beta < -1$.

3 DISSIPATION IN A RELATIVISTIC OUTFLOW

We consider the evolution of a cold, mildly magnetized, expanding spherical shell coasting at a constant $\Gamma = (1-\beta^2)^{-1/2}$ with a constant lab-frame radial width Δ. At a lab-frame time t the front edge of the ejecta shell is at a radial distance $R = \beta ct$ from the central source. Following the relation given in equation (1), the dissipation episode is assumed to start at $R = R_0 = 6\times10^{13}\Gamma_2^2$ cm (for brevity, hereafter estimates are given for fixed intrinsic parameters: $L_{52} = 100$, $T_{v,-1} = 1$, magnetization $\sigma = 0.1$, electron fraction $Y_{\rm e} = 0.5$, but show the explicit dependence on Γ) and end at $R = R_{\rm f} = R_0 + \Delta R$ with $\Delta R = R_0$, i.e. after one dynamical time, but the shell can still radiate also at $R > R_{\rm f}$. The rise and decay times of the resulting pulse in the GRB light curve are $t_{\rm rise} \simeq \Delta R/2c\Gamma^2$ and $t_{\rm decay} \simeq R_{\rm f}/2c\Gamma^2$, so one can in principle use this to determine both R_0 and ΔR if Γ can be independently inferred. The outflow carries a magnetic field of comoving strength $B' \approx 4\times10^5\Gamma_2^{-3}$ G and kinetic energy dominated by baryons.

Depending on the efficiency of the dissipation mechanism, a fraction $\varepsilon_{\rm rad} = 0.5$ of the total power L_j carried by the outflow is converted into radiation, such that the observed isotropic-equivalent luminosity is $L = \varepsilon_{\rm rad}L_j = L_{52}10^{52}\,{\rm erg\,s^{-1}}$. This corresponds to a comoving compactness $\ell'_0 \approx 2.7\times10^4\Gamma_2^{-5}$ at the dissipation radius R_0. The initial Thomson scattering optical depth of baryonic electrons is $\tau_{\rm T_0} \approx 18\Gamma_2^{-5}$. A fraction $\varepsilon_{\rm nth} \approx 0.87\Gamma_2^{-1}$ of which have $\tau_{\rm T,nth}$ and are assumed to be accelerated to a power-law energy distribution, $n'_{\rm e}(\gamma_{\rm e}) \propto \gamma_{\rm e}^{-q}$ for $\gamma_{\rm m} < \gamma_{\rm e} < \gamma_{\rm M}$, with $\langle\gamma_{\rm e}\rangle_{\rm nth}$ chosen so that the pitch angle averaged synchrotron peak energy of fast cooling electrons yields $E_{{\rm p},z} = (1+z)E_{\rm pk} = \Gamma E'_{\rm pk} = 500E_{\rm p,2.7}$ keV. The relativistically hot electrons are injected with constant power L, and then loose all their energy to synchrotron radiation and inverse-Compton scattering (ICS) of soft seed photons to high energies. The remaining fraction $1-\varepsilon_{\rm nth}$ of baryonic electrons with Thomson optical depth $\tau_{\rm T,th}$ stay cold ($k_{\rm B}T'/m_{\rm e}c^2 \equiv \theta' = 10^{-2}$) and form a thermal distribution. The full details of the model will be provided elsewhere (Gill & Granot 2017, in preparation).

3.1 Effect of thermal Comptonization and pair annihilation on $x_{\rm c}$ in the Thomson-thick regime

In a single ICS event, the energy of a soft seed photon (x'_0) is amplified by a constant factor, such that the scattered photon has energy $x' = (1+A)x'_0$. For ultrarelativistic electrons with $\gamma_{\rm e} \gg 1$, the mean fractional change in the seed photon's energy is $A = \frac{4}{3}\gamma_{\rm e}^2$ in the Thomson-limit ($x'_0\gamma_{\rm e} < 1$). If the scattering electrons have a Maxwellian distribution with temperature θ', then thermal Comptonization yields (when neglecting downscattering) $A = 16\theta'^2 + 4\theta'$ (e.g. Rybicki & Lightman 1979; Pozdnyakov, Sobol' & Sunyaev 1983), which is valid for both non-relativistic ($\theta' < 1$) and relativistic ($\theta' > 1$) electrons. The importance of multiple ICSs in modifying the seed spectrum is gauged by the magnitude of the Compton parameter,[2] $y_{\rm C} = A\tau_{\rm T}$, where $\tau_{\rm T}$ is the electron Thomson optical depth. After multiple scatterings, upon its escape, the seed photon's energy is amplified to $x'_{\rm f} \sim x'_0 e^{y_{\rm C}}$ (for $x'_{\rm f} \ll 4\theta'$). Thus, when $y_{\rm C} > 1$ and $\tau_{\rm T} > 1$ Comptonization becomes important, and for $y_{\rm C} \gg 1$ it 'saturates' and forms a Wien peak at $x'_{\rm W} = 3\theta'$.

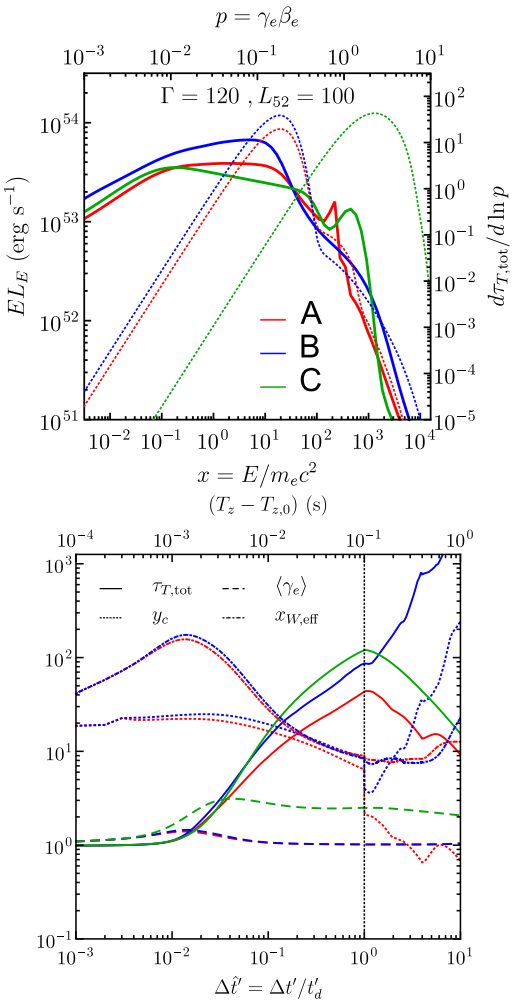

Figure 2. (Top): CEF spectrum from a spherical shell (solid) and corresponding electron energy distribution (dotted) after one dynamical time, $\Delta t' = t'_{\rm d} = R_0/\Gamma c \Leftrightarrow \Delta T_z = T_v$, for three cases: (A) all processes turned on, (B) no PA, and (C) no Compton scattering. (Bottom): Time evolution of some key parameters: the total Thomson depth $\tau_{\rm T,tot} = \tau_{\rm T,th} + \tau_{\rm T,nth} + \tau_{\rm T,\pm}$, Compton $y_{\rm C}$ parameter, average Lorentz factor of $e^\pm$-pairs $\langle\gamma_{\rm e}\rangle$, and the effective energy of the Wien peak $x_{\rm W,eff}$.

Fig. 2 shows the CEF spectrum at the end of one dynamical time (top-panel), stressing the spectral changes brought by Comptonization and PA. The corresponding electron energy distribution is predominantly thermal in all three cases due to the high total $\tau_{\rm T,tot} = \tau_{\rm T,th} + \tau_{\rm T,nth} + \tau_{\rm T,\pm}$ (lower panel). Initially, $\tau_{\rm T,tot} = \tau_{\rm T,th} = (1-\varepsilon_{\rm nth})\tau_{\rm T_0} \approx 1$ which builds up over the dynamical time, $t'_{\rm d} = R_0/\Gamma c$, due to injection of relativistic electrons and

[2] Usually, $\max(\tau_{\rm T}, \tau_{\rm T}^2)$ is taken for the mean number of scatterings $N_{\rm sc}$ instead of $\tau_{\rm T}$, but here $\tau_{\rm T} \propto R^{-2}$ due to the shell's expansion so that $N_{\rm sc} \sim \tau_{\rm T_0}$ as it is dominated by the first dynamical (or radius-doubling) time.

Downloaded from https://academic.oup.com/mnrasl/article-abstract/475/1/L1/4693845
by OPEN UNIVERSITY user
on 17 January 2018

subsequent production of $e^{\pm}$-pairs that dominate $\tau_{\rm T,tot}$, when $\ell' \gg 1$. It suffers a sharp decline at $\Delta t' = t'_{\rm d}$ after which injection of electrons ceases and the hot pairs cool and annihilate with the thermal pairs. This is not so when PA is turned off. In all cases (except with no ICS), $y_{\rm C} \gg 1$ which results in saturated Comptonization. The position of the Wien peak in the observer frame is obtained from $x_{\rm W} \simeq 2\Gamma x'_{\rm W} = 6\Gamma\theta'$ (the factor of 2 results from higher weight given to on-axis ($\theta_\Gamma = 0$) emission upon integration over the equal arrival time surface (Granot, Piran & Sari 1999) since $L/L' = \delta_{\rm D}^4$, where $\delta_{\rm D} \approx 2\Gamma/[1 + (\Gamma\theta_\Gamma)^2)]$ is the Doppler factor and θ_Γ is the angle measured from the line of sight).

The temperature of the thermal pairs is related to their mean energy, $\langle\gamma_{\rm e}\rangle = [3\theta' K_2(1/\theta') + K_1(1/\theta')]/[2\theta' K_1(1/\theta') + K_0(1/\theta')]$ (Pozdnyakov, Sobol' & Sunyaev 1983), where K_n are the modified Bessel functions of the second kind. Since at early times the particle distribution is quasi-thermal that transforms into predominantly thermal over time, the $\langle\gamma_{\rm e}\rangle - \theta'$ relation only yields the 'effective' temperature of the $e^{\pm}$-pairs, and consequently an effective energy for the Wien peak ($x_{\rm W,eff}$). At the end of the dynamical time, when $\tau_{\rm T} \gg 1$, this approximation becomes more exact as the particles and photons come into thermal equilibrium. When Compton cooling of the injected relativistic electrons and mildly relativistic $e^{\pm}$-pairs is switched off, the hot particles share their energy with the much cooler thermal (baryonic) electron distribution via Coulomb interactions. This has the effect of heating up the thermal distribution which yields higher particle temperatures by the end of the dynamical time and broadens the PA line. In contrast, ICS of hot electrons on soft synchrotron photons helps regulate the temperature of the particle distribution to much lower ($\theta' < 1$) values, which also yields a much sharper annihilation feature.

How far below unity can the temperature of a pair-dominated plasma drop? Many works have tried to understand thermal pair equilibria of mildly relativistic (Svensson 1984) and relativistic plasmas (Lightman 1982; Svensson 1982). By solving the pair balance equation, where pair production balances PA in steady-state, it was realized that no equilibrium exists for $\theta' > \theta'_{\rm max} = 24$, when $\ell' \ll 1$ and for $\theta' \gtrsim 0.4$, when $\ell' > \ell_{\rm WE}(\theta') \gg 1$ (Svensson 1984). At $\ell' \gg 1$, when Comptonization dominates over photon emission/absorption and escape, the pairs establish a Wien equilibrium where the compactness of the radiation field depends uniquely on the pair temperature for $\theta' \lesssim 0.4$, such that $\ell'_{\rm WE}(\theta') = 4\sqrt{2\pi}\theta'^{5/2}\exp(1/\theta')$ (Svensson 1984). Hence, the temperature of the non-relativistic thermal pairs decreases below unity logarithmically with ℓ'. This trend continues until a local thermodynamic equilibrium is established due to true photon emission/absorption processes (e.g. cyclo-synchrotron emission and self-absorption).

From the condition of pair equilibrium, the relation between ℓ' and $\tau_{\rm T,\pm}$ can be obtained when $\ell' \gg 1$. Under the assumption that all of the injected energy at this stage goes into producing hard photons ($x' > 1$) that can annihilate with other soft ($x' < 1$) photons as well as self-annihilate, the rate of pair production is $\dot{n}'_+ = L/(4\pi R^3 \Gamma m_{\rm e} c^2) = c\Gamma^2\ell'/\sigma_{\rm T} R^2$. These pairs then annihilate the cooler thermal pairs at the rate $\dot{n}'_{\rm A} \sim \sigma_{\rm T} c n'^2_+$. In equilibrium $\dot{n}'_+ = \dot{n}'_{\rm A}$, which yields up to a factor of order unity $\tau_{\rm T,\pm,eq} \sim \sqrt{\ell'_0}(R_0/R)$ (e.g. Pe'er & Waxman 2004), where the density dilution due to expansion is reflected by the ratio of radii. In the top panel of Fig. 3, we show $\tau_{\rm T,\pm,eq}$ along with the total Thomson depth of particles, which is dominated by that of pairs, at the end of a dynamical time from simulations without PA and Compton scattering. We find that $\tau_{\rm T,tot} \approx \tau_{\rm T,\pm} \sim \tau_{\rm T,\pm,eq}$ for $\ell' \gg 1$, when all radiative processes are included. The agreement is approximate since the pair-photon plasma hasn't established a steady state. When PA is switched off, we find $\tilde{\tau}_{\rm T,tot} \approx 2\tau_{\rm T,tot}$ after one dynamical time over a wide range of compactness.

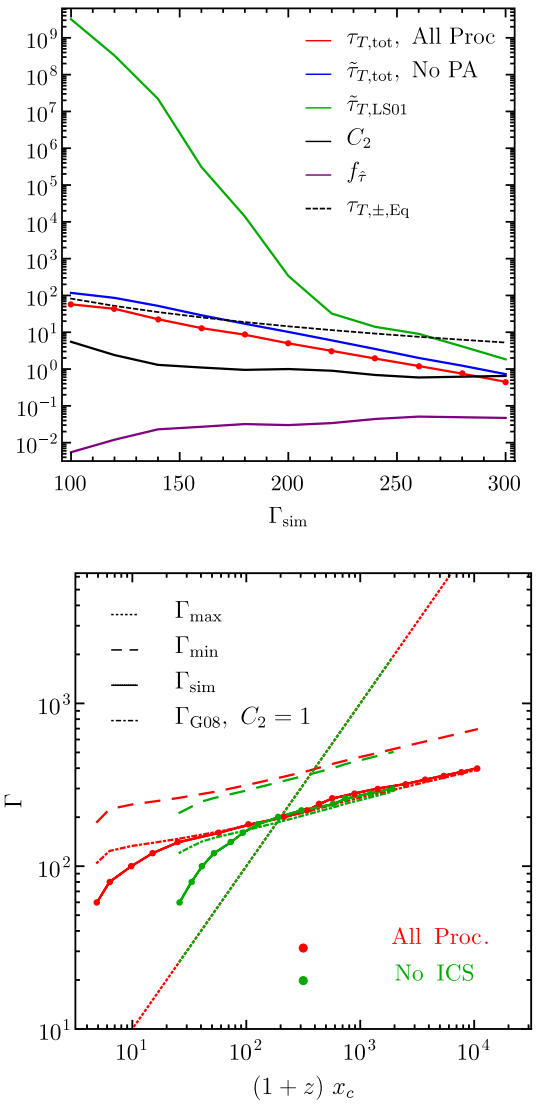

Figure 3. (**Top**) Comparison of the Thomson depth from simulations with all processes active and with no PA to that obtained from the analytic model of LS01. See text for definition of all quantities. (**Bottom**) Comparison of Γ from the simulation $\Gamma_{\rm sim}(x_c)$ to the prediction of the LS01 analytical model $\Gamma_{\rm min}(x_c)$ and $\Gamma_{\rm max} = (1+z)x_c$ (compare with Fig. 1). Γ predicted by equation (126) of G08 ($\Gamma_{\rm G08}$) for $C_2 = 1$ is also shown.

3.2 Comparison with one-zone analytic model predictions

Earlier we outlined two regimes of the one-zone analytic model of LS01 which did not account for annihilation of $e^{\pm}$-pairs. Here, we compare the results of our simulations to the predictions of LS01. First, we need to determine the position of the high-energy cut-off, which along with other spectral parameters such as the high-energy spectral slope and normalization, yields an estimate of Γ. We obtain the position of the cut-off energy in the CEF by fitting the spectrum to a Band function (Band et al. 1993) with a broken power-law high-energy cut-off (see equation E5 of Vianello et al. 2017).

In Fig. 3, we compare the results obtained from the simulations to the predictions of the LS01 analytic model and equation (126) of

Downloaded from https://academic.oup.com/mnrasl/article-abstract/475/1/L1/4693845
by OPEN UNIVERSITY user
on 17 January 2018

G08. We find that the LS01 model grossly overpredicts the Thomson scattering depth of pairs in the Thomson-thick regime. In the Thomson-thin regime, $\tilde{\tau}_{\rm T,LS01}$ asymptotically approaches $\tilde{\tau}_{\rm T,tot}$ in Fig. 3 since the analytical model does not account for PA. In addition, the LS01 model also finds $\Gamma_{\rm min}$ to be a factor $\sim$2 larger than the simulated value $\Gamma_{\rm sim}$. This result is consistent with the work of Vianello et al. (2017), where they compare Γ obtained from the models of G08 and Gill & Thompson (2014) that self-consistently produce high-energy spectral breaks to that predicted by the LS01 model for GRBs 100724B and 160509A. The predictions of LS01 can be reconciled with the simulation results by renormalizing $\hat{\tau} \rightarrow f_{\hat{\tau}}\hat{\tau}$ in equation (4), where $f_{\hat{\tau}} \equiv \hat{\tau}_{\rm sim}/\hat{\tau}_{\rm LS01}$. This ratio is shown in Fig. 3, where $f_{\hat{\tau}} \sim 0.05$ for $\Gamma > 100$.

The main effect of Compton scattering (see Fig. 3) is that $x_{\rm c}$ becomes lower due to downscattering of energetic photons with $x' > 4\theta'$ by cold thermal $e^{\pm}$ pairs. We find good agreement between $\Gamma_{\rm sim}$ and $\Gamma_{\rm G08}$ in the Thomson-thin regime for $C_2 = 1$, where C_2 is an order unity parameter in equation (126) of G08 whose exact value is determined numerically. When ICS is switched on, we find $C_2 \sim 0.5 - 1$ in order for $\Gamma_{\rm G08} = \Gamma_{\rm sim}$, which is consistent with the results of Vianello et al. (2017); $\Gamma_{\rm G08}$ deviates only slightly (factor of $\sim$2) deep in the Thomson-thick regime and remains a reliable estimator of the true Γ for $\Gamma_{\rm max} \gtrsim 0.1\Gamma_{\rm tr,G08} \Leftrightarrow x_{\rm c} \gtrsim 0.1x_{\rm tr,G08}$, where $\Gamma_{\rm tr,G08} = (1+z)x_{\rm tr,G08}$ and $x_{\rm tr,G08}$ are defined as the point where $\Gamma_{\rm G08} = \Gamma_{\rm max}$.

Most importantly, the break in $\Gamma(x_{\rm c})$ at $x_{\rm c} = x_{\rm tr}$ predicted by the LS01 model is shifted to lower energies both when ICS is on and off, where ICS shifts the break to even lower energies. Also, the slope in the Thomson-thick regime is different in the two cases. In that regime, if the photo-pair-plasma has achieved steady-state and manifests a Wien-peak then the $\ell'_{\rm WE} - \theta'$ relation can be used to determine $\Gamma(x_{\rm c})$. Since neither of the two conditions are fulfilled here this relation is invalid. In the absence of ICS, when no downscattering of photons occurs, we find that $\Gamma_{\rm sim}(x_{\rm c})$ asymptotically approaches $2\Gamma_{\rm max}(x_{\rm c})$ in the Thomson-thick regime when $\ell' \gg 1$.

4 IMPLICATIONS AND DISCUSSION

In many works (e.g. Tang et al. 2015) that find the spectral cut-off to lie in the Thomson-thick regime, Γ is estimated using $\Gamma_{\rm max}$. It is clear from Fig. 3 that this approach can lead to erroneous results and can underestimate Γ by as much as an order of magnitude when $\ell' \gg 1$. This result is quite general such that it doesn't depend on the details of any particular GRB model, but only on the compactness of the dissipation region that is set by a combination of three intrinsic parameters: L, Γ, R.

In the Thomson-thin regime, the simple analytic model overpredicts Γ by a factor of $\sim$2 (G08; Hascoët et al. 2012). This work shows that the effect of pair cascades on the high-energy spectral cut-off cannot be ignored and, more importantly, a model employing the time-dependent evolution of the spectrum must be used to obtain an accurate estimate of Γ. The simple one-zone analytical models lack the requisite complexity to accurately predict Γ.

In this work, the cut-off energy is determined for a single pulse after integrating the spectrum over the equal arrival time surface. Generally, due to poor photon statistics, observations use several overlapping pulses emerging from different parts of the outflow with an order unity spread in Γ. This introduces some smearing of the cut-off energy and sharp annihilation line within a single pulse as well as over several adjoining pulses.

The simple one-zone analytic models of e.g. LS01, Abdo et al. (2009b) disagree with the more detailed analytic work of G08 and the results presented here due to the following main reasons. (i) They only use the power-law component of the Band function rather than the smoothly broken power law at $x < x_{\rm pk}$ [however, see for e.g. Gupta & Zhang 2008; although G08 also uses an infinite power law but see (ii)]. For typical spectral indices $\alpha \sim -1$ and $\beta \sim -2$ below and above $x_{\rm pk}$, respectively, the number of photons in an infinite power law is larger by a factor of $x_{\rm pk}/[x\log(x/x_{\rm pk})]$ for $x < x_{\rm pk}$ as compared to the Band function. This decrement in photon number reduces $\tau_{\gamma\gamma}$ seen by hard photons with $x > 1/x_{\rm pk}$. Consequently, the estimated Γ is lower. (ii) The assumption of (comoving) isotropy of the radiation field in such models yields higher estimates of Γ. The effect of an anisotropic radiation field is to increase the threshold for pair production and decrease the rate of interaction due to the typical angle of interaction between photons $\theta_{12} \sim 1/\Gamma$. This effect is included in G08 which generally finds a lower Γ. (iii) All analytic models neglect the effect of pair cascades, which becomes very important in the Thomson-thick regime.

ACKNOWLEDGEMENTS

RG and JG acknowledge support from the Israeli Science Foundation under grant no. 719/14. RG is supported by an Open University of Israel Research Fellowship.

REFERENCES

Abdo A. A. et al., 2009, Science, 323, 1688
Ackermann M. et al., 2011, ApJ, 729, 114
Band D. et al., 1993, ApJ, 413, 281
Baring M. G., 2006, ApJ, 650, 1004
Baring M. G., Harding A. K., 1997, ApJ, 491, 663
Fenimore E. E., Epstein R. I., Ho C., 1993, A&AS, 97, 59
Fishman G. J., Meegan C. A., 1995, ARA&A, 33, 415
Gill R., Thompson C., 2014, ApJ, 796, 81
Goodman J., 1986, ApJ, 308, L47
Granot J., Piran T., Sari R., 1999, ApJ, 513, 679
Granot J., Cohen-Tanugi J., do Couto E Silva E., 2008, ApJ, 677, 92 (G08)
Guilbert P. W., Fabian A. C., Rees M. J., 1983, MNRAS, 205, 593
Gupta N., Zhang B., 2008, MNRAS, 384, L11
Hascoët, Daigne F., Mochkovitch R., Vennin V., 2012, MNRAS, 421, 525
Kumar P., Zhang B., 2015, Phys. Rep., 561, 1
Lightman A. P., 1982, ApJ, 253, 842
Lithwick Y., Sari R., 2001, ApJ, 555, 540
Murase K., Ioka K., 2008, ApJ, 676, 1123
Paczyński B., 1986, ApJ, 308, L43
Pe'er A., Waxman E., 2004, ApJ, 613, 448
Pe'er A., Waxman E., 2005, ApJ, 628, 857
Piran T., 1999, Phys. Rep., 314, 575
Pozdnyakov L. A., Sobol' I. M., Sunyaev R. A., 1983, SPRv, 2, 189
Razzaque S., Mészáros P., Zhang B., 2004, ApJ, 613, 1072
Rees M. J., Mészáros P., 1992, MNRAS, 258, 41
Ruderman M., 1975, Ann. NY Acad. Sci. 262, 164
Rybicki G. B., Lightman A. P., 1979, Wiley-Interscience, New York
Svensson R., 1982, ApJ, 258, 335
Svensson R., 1984, MNRAS, 209, 175
Tang Q.-W., Peng F.-K., Wang X.-Y., Tam P.-H. T., (2015), ApJ, 806, 194
Thompson C., 1994, MNRAS, 270, 480
Vianello G. et al., 2017, ApJ, preprint (arXiv:1706.01481)
Vurm I., Beloborodov A. M., Poutanen J. ApJ, 738, 77
Woods E., Loeb A., 1995, ApJ, 453, 583

This paper has been typeset from a TEX/LATEX file prepared by the author.

Downloaded from https://academic.oup.com/mnrasl/article-abstract/475/1/L1/4693845
by OPEN UNIVERSITY user
on 17 January 2018